Automated Optic Nerve Head Detection in Fluorescein Angiography Fundus Images

M. Tavakoli, M. H. Bahreini Toosi, R. Pourreza, T. Banaee, H. R. Pourreza

Abstract– **The identification of the optic nerve head (ONH) is necessary preprocessing step in retinal image analysis, for automated extraction of the anatomical components in retinal images. In this study, a new image processing method based on Radon transform (RT) and multi-overlapping windows was proposed for ONH detection in fluorescein angiography (FA) fundus images. At first, RT was applied to all fundus sub images to find candidates for the location of the ONH. Then, the accurate location was found using the minimum mean square error estimation. The results of our automated method for the ONH detection in the images showed sensitivity and specificity of 90.54%, 98.51% respectively for pixel based analysis, and according to manual ONH detection, our automated algorithm found 89 ONH out of 100 in true location for FA images. This study addresses a novel method in detection of retinal land marks. Sensitivity and specificity of this algorithm seems to be acceptable in comparison with other detection methods.**

I. INTRODUCTION

AUTOMATED diagnosis programs for retinopathy are largely used in worldwide. An important benefit of automated or Computer Assisted Diagnosis (CAD) systems is the accurate detection or localization of main anatomical landmarks and lesions in the image. In addition, the computer techniques are applied for providing physicians assistance at any time and to relieve their work load or iterative works.

Identification of the optic nerve head (ONH) is one of the most important issues in retinal image analysis. The ONH segmentation is a critical preprocessing step in many methods and algorithms designed for the automatic extraction of retinal landmarks and lesions [1].

The ONH is yellowish region in color fundus image that usually occupied one seventh of fundus image [2]. The main characteristic of ONH is rapid intensity changing due to dark blood vessels that are in vicinity of bright ONH. This intensity alteration is characteristic of interest for ONH recognition. The ONH have three properties in order to be localized: (1) ONH appears as a bright disk nearly 1600μm in diameter, (2) entering of the large blood vessels from above and blew, and (3) blood vessels diverge from ONH.

In many algorithms, ONH diameter is used as a length reference to measure objects in retina [1, 3]. High intensity variation of ONH could interfere with some segmentation algorithm thus, sometimes it is necessary to detect and mask it to promote the result of segmentation process. On the other hand, the ONH is initial step for retinal vessel segmentation methods [3]. That means, large vessels found in the neighbor of ONH are a sign for vessel tracking techniques.

In CAD systems point of view, detection of ONH plays a critical role in developing automated diagnosis systems of some diseases like diabetic retinopathy (DR). The relatively constant distance between the ONH and the fovea, can be used to help estimate the location of the latter [2]. Identifying and masking the ONH improves the classification of exudates regions in images with DR and decrease false positive rate in the detection of regions with retinal exudates [4]. But identification of the ONH is difficult because of discontinuity of its boundary, due to crossing large vessels as well as considerable color or intensity change in other parts of retinal image because of some pathologies (such as exudates) [5].

II. MATERIAL AND METHOD

In this study a Radon transform (RT) based algorithm was proposed for detection of ONH in fundal images. Between detector algorithms, the RT is less sensitive to noise in the image than others, because the intensity variations due to noise tend to be omitted by the process of integration. In the proposed algorithm fundal image was first partitioned into some overlapping blocks or windows. Local RT was then applied to each block. The peak of sub-image in Radon space would be associated with the ONH (if ONH lays in the sub-image). The sub-image which included the peak was further analyzed for ONH presence validation. The algorithm output was a mask for ONH.

Our automated system has been developed using MUMS-DB (**M**ashhad **U**niversity **M**edical **S**cience **Data**base) consisted of normal and diabetic fluorescein angiography (FA) retinal images, which were acquired in the Khatam-Al-Anbiya Eye Hospital. Image distribution did not correspond to any typical population, i.e., the data was biased and no priori information can be devised from it. All images were obtained using 50° retinal camera. Images were usually obtained from the posterior pole's view including optic disc and macula. The

Manuscript received November 4, 2011.

Meysam Tavakoli is with the Center for research in Medical Physics and Biomedical Imaging from Mashhad University of Medical Sciences. (Corresponding author to provide Tel/fax: +982144336775; email: MeysamTavakkoli@gmail.com)

Hamidreza Pourreza and Reza Pourreza are with the Computer Engineering Department, Ferdowsi University of Mashhad, Iran (Email: hpourreza@um.ac.ir , pourreza.reza@yahoo.com)

Mohammad Hosein Bahreini Toosi is with the Department of Medical Physics, Mashhad University of Medical Sciences, School of Medicine. (Email: Bahreinimh@mums.ac.ir)

Touka Banaee is with the Ophthalmic Research Center, Khatam-Al-Anbia Hospital, Mashhad University of Medical Sciences, Mashhad, Iran. (Email: banaeet@mums.ac.ir)

acquired image resolution is 2896 × 1944 in 24bit Tag Image File Format (TIFF). We used a set of 100 images, including 80 cases in different stage (4 stages) of DR as case group, and 20 without DR.

We asked an expert ophthalmologist to mark the ONH and its boundary in these 100 images using added transparent layer on images. ONH location and its boundary according to her detection save in a similar size files called ground truth file make our gold standard in this project. Ground truth files of selected fundus images from MUMS-DB were also collected in it.

A. *Radon transform*

The RT is at the center of the mathematical model for the measurements made in x-ray computed tomography (CT). Therefore, one of the most influential examples in applications of computer assisted tomography happens in diagnostic medicine, where the method is applied to produce images of the interior of human organs.

A projection of a 2D function *f(x, y)* is a set of line integrals. The Radon function computes the line integrals from multiple sources along parallel paths, or beams, in a certain direction. The beams are spaced 1 pixel unit apart. To represent an image, the Radon function takes multiple, parallel-beam projections of the image from different angles by rotating the source around the center of the image.

We define the RT of a function *f* on the plane by:

$$\check{R}_{\theta}(s) = \int\int R(x,y)\, \delta(s - x\cos\Theta - y\sin\Theta)\, dx\, dy \qquad (1)$$

In CT scan, the data needed to reconstruct the image are transmission measurements through the patient. A single projection of the object $\check{R}_{\theta}(s)$ is defined as equation (1). Where, the Dirac delta function δ picks out the path of the line integral.
Equation (1) expresses the linear relationship between the object function f (x, y) and the measured projection data $\check{R}_{\theta}(s)$. The quantity $\check{R}_{\theta}(s)$ in (1) may be interpreted as the one-dimensional function $\check{R}_{\theta}(s)$ of a single variable s with θ as a parameter; this $\check{R}_{\theta}(s)$ is referred to as a parallel projection.

The RT is able to transform circular pattern or discontinued points to a line in Radon space and could easily distinguish from other patterns.

B. *Multi-overlapping window*

In the proposed algorithm fundus image was partitioned into overlapping widows. To find objects on border of sub-images, we have to define an overlapping pattern of sliding windows. To determine the size of each sub-image or sliding window, we used our knowledge database. In this regard, size of targeted object specified the size of the windows (*n*).

The windows overlapping ratio was another important parameter which affected the algorithm's performance. If window's step is equal to one, we will search every pixel of images just one time and sub-images only touch each other without any overlapping and if step is defined as two or more, then we go (*n/step*) pixel each time either in horizontal or vertical sliding then each pixel would belong to up to n^2 sub-images. (See Fig. 1) Thus in the proposed system a parameter *step* is used which defines the adjacent windows overlapping ratio.

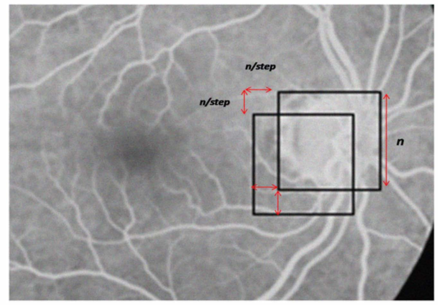

Fig. 1. Window size and overlapping ratio (n, step).

III. Detection of the ONH

ONH is characterized as a bright circular object set against a background and because of large vessels coming out and going in through it; its edges are ill defined. ONHs are non-uniform in intensity, size, and location.

Our algorithm, for ONH detection in FA fundus images, was composed of 4 steps:

1. Generation of sub-images
2. Applying Local Radon Transform
3. ONH Certifying
4. ONH mask

A RT based approach for extraction of ONH in addition to, the utilized technique for ONH detection simplifies the procedure of ONH detection for the input retinal image.

A. *Generation of sub-images*

The ONH should be extracted in local windows. The window size (*n*) has a direct effect on the extraction accuracy.

A small/large *n* would lead to extract other bright pattern like MAs or scar tissue while ONH would not be extracted. ONH can be extracted by adjusting the *n* value. Based on our knowledge about the ONH size and its maximum diameter, appropriate *n* was selected. In this manner, the size of *n* is chosen equal to maximum diameter of ONH in pixel (n=79 pixels). Another important parameter is the windows overlapping ratio. The speed of algorithm depends on the rate of *step*. In other words, if we increase the *step* the computation burden of algorithm is increased exponentially and vice versa. In the proposed system a parameter *step* is used which defines the adjacent windows overlapping ratio. Fig. 4 depicts the relation of *step* and window size (*n*). In this study the optimum of step was selected 4 pixels empirically.

B. *Applying Local Radon Transform*

High intensity between ONH and image background in FA images causes the ONH to be associated with peaks in Radon space. After generating the sub-images into windows or blocks, local RT is applied to the masked image (again equation 1).

In our case both x and y, in (1), are equal to n. The amplitude of projection in diagonal directions ($\theta=45^{\circ}$, $\theta=135^{\circ}$, $s=n\sqrt{2}$) is higher than other directions, thus the peak of RT is more likely to happen in diagonal directions. To eliminate the diagonal effect, the input sub-image is firstly masked using a circle. The masking process is shown in Fig. 2.

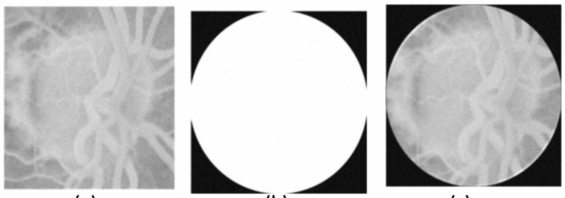

(a) (b) (c)

Fig. 2. Masking process. (a) Original sub-image; (b) applied mask; (c) masked sub-image.

As mentioned before, ONH in a sub-image was associated with a prominent peak in Radon space; therefore at this stage peaks should be detected.

The peak was detected in the Radon space. Profiles in which peak occurred, were candidates that might contain ONH. These profiles were further analyzed for validation of candidate ONH.

C. ONH Certifying

The main concept of this section was similar to peak measuring in all projection angles in Radon transformation of a sub-image with a central point pattern. By this simple assumption we compared all sub-images which have a peak profile higher than a predefined threshold.

For detection of correct ONH, we used RT property for round objects. For a round object, RT results are same profiles in all directions. Due to roundness of ONH, profiles related to projections have minimum deviation with each other; therefore we can detect that sub-image contain ONH with this procedure. To achieve this goal, mean square error between projections was calculated. In other words, we found the sub-image which minimizes the mean square error between all of its different projections. (Fig. 3)

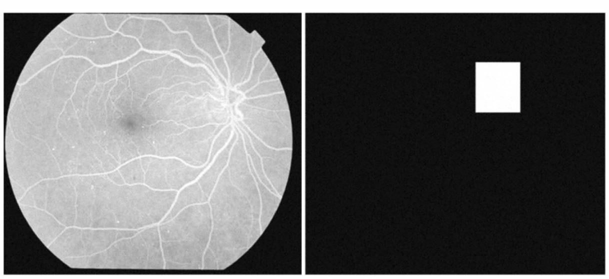

(a) (b)

Fig. 3. (a) Original fluorescein angiography fundus image from MUMS-DB, (b) its validate ONH sub-image.

D. ONH mask

ONH detection and its changes are very important in some pathologic conditions. Contrast variance of ONH, could make some artifact in all image segmentation methods working on fundus images, thus it is necessary to find ONH and mask it. After validation of ONH by the described methods, the center of sub-image which was contacted the ONH considering as the center of a circular mask for ONH. The diameter of the mask was calculated by the maximum possible diameter of ONH according to our image capturing resolution.

Fig. 4 shows sample result in FA fundus image. The acquired result demonstrates the high accuracy of the proposed algorithm in extraction of ONH.

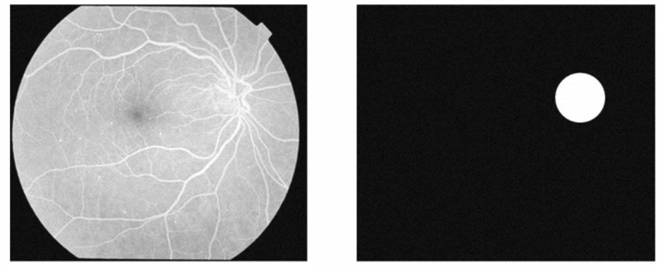

(a) (b)

Fig. 4. (a) Original FA fundus image from MUMS-DB, (b) ONH mask related to this image.

In the final section, statistical information about the sensitivity and specificity measures is extracted. The higher the sensitivity and specificity values, the better the procedure. Sensitivity and specificity values can be calculated as follows.

$$Sensitivity\ (S_N) = TP/\ (TP+FN) \qquad (2)$$

$$Specificity\ (S_P) = TN/\ (TN+FP) \qquad (3)$$

IV. Results

For 100 images of test set, our reader labeled the ONH on the images and the result of this manual segmentation were saved to be analyzed further. According to manual ONH detection our automated algorithm founded 89 of ONH in true location in FA images.

Another analysis made by comparing the result of automated detection with hand labeled ONH in pixel base method. If any pixel belongs to the ONH detected in automated algorithm, it considers TP, any ONH pixels which are not detected in automatic method considers as FN, and other pixels out of the ONH labeled area consider as FP if they consider as ONH area in our method and all pixels out of the ONH area which are belongs to fundus image consider as TN when the automatic method did not mark them as ONH area.

The results of pixel base analysis are shown in two below tables.

TABLE I
RESULTS OF ONH DETECTION IN FA IMAGES

	TP	FP	TN	FN
Pixel based	3,770,712	3,192,211	558,913,363	298,325
Sensitivity		92.66%		
Specificity		99.43%		

V. Discussion and Conclusion

A potential use of fundal digital image analysis is the ability to analyze large fundal images in a short period of time without tiredness. The identification of fundal landmark features such as the ONH, fovea and the retinal vessels as reference coordinates is a prerequisite before systems can do more complex tasks identifying pathological entities. Reliable techniques exist for identification of these structures in retinal photographs.

Since fundus images are nowadays in digital format, it is possible to create a computer-based system that automatically detects abnormal lesions and landmarks from fundus images. An automatic system would save the workload of well-paid ophthalmologists, and letting hospitals and eye clinics to use their resources in other important tasks. It could also be possible to screen more people and more often with the help of an automated system, since it would be more inexpensive than screening by humans.

In this study an automated algorithm were utilized for ONH detection without intervention of any ophthalmologist. We presented the segmentation of the ONH by using of combination of RT and multi-overlapping window. As we said before, the RT makes our algorithm more robust and less sensitive to noise than other proposed algorithms. The quality of our identification depends on some parameters such as the length of our window (n), measure of step, thresholding validation, etc. Besides set of images is completely independent and select randomly.

The results presented in this study show that the proposed technique is reliable and robust in ONH segmentation. Our algorithm detected correctly 89% of ONH in FA images. Another evaluation of our algorithm is related to pixel base analysis. In this manner, we reached to sensitivity and specificity of 92.66%, 99.43% for FA images respectively in pixel base analysis.

Related to some other works, as we said Sinthanayothin et al. [2] detected ONH but others have found that their algorithm often fails for fundus images with a large number of white lesions, light artifacts or strongly visible choroidal vessels [6]. Others had exploited the Hough transform to locate the ONH [5]. However, Hough spaces tend to be sensitive to the chosen image resolution [7].

On the other hand, even the ONH segmentation is useful for automated diagnosis of other ophthalmic pathologies such as glaucoma [8]. Glaucoma is the second most important cause of blindness in the world [9]. Therefore, ONH detection and analysis can effect to detect evidence of automatic detection of Glaucoma.

The goal of this work was to develop algorithms for detecting ONH in FA fundus images. Our algorithm has some important characteristics in detection ONH in retinal images that include:

1. The algorithm was not based on tracking vessel in order to find ONH.
2. The algorithm was robust to noise because of its linear integral transformation concept.
3. Combination of two methods (Radon transform and multi-overlapping window) made performance of algorithm acceptable in detection ONH.

We conclude that RT based ONH detection is an effective method in color and FA fundus images even in the presence of DR related lesion like exudates.

Acknowledgment

The authors acknowledge support for a Master degree grant No. 87394 from Mashhad University of Medical Science (MUMS).

References

[1] L. Gagnon, M. Lalonde, M. Beaulieu, and M. C. Boucher, "Procedure to detect anatomical structures in optical fundus images," in *Proc. Conf. Med. Imag. 2001: Image Process.*, San Diego, CA, 2001, pp. 1218–1225.

[2] C. Sinthanayothin, J. F. Boyce, H. L. Cook, and T. H. Williamson, "Automated localisation of the optic disc, fovea, and retinal blood vessels from digital colour fundus images," *Br. J. Ophthalmol.*, vol. 83, no. 8, pp. 902-910, 1999.

[3] A. Osareh, M. Mirmehdi, B. Thomas, R. Markham, Classification and localisation of diabetic-related eye disease, in: Proceedings of the 7th European Conference on Computer Vision (ECCV), vol. 2353, 2002, pp. 502–516.

[4] A. Osareh, M. Mirmehdi, B. Thomas, and R. Markham, "Automated identification of diabetic retinal exudates in digital colour images," *Br. J. Ophthalmol.*, vol. 87, pp. 1220–1223, 2003.

[5] B. Kochner, D. Schuhmann, M. Michaelis, G. Mann, and K. H. Englmeier, "Course tracking and contour extraction of retinal vessels from color fundus photographs: Most efficient use of steerable filters for model-based image analysis," *in Proc. SPIE Med. Imag.*, 1998, pp. 755–761.

[6] J. Lowell, A. Hunter, D. Steel, A. Basu, R. Ryder, E. Fletcher, and L. Kennedy, "Optic nerve head segmentation," *IEEE Trans. Med. Imag.*, vol. 23, no. 2, pp. 256–264, Feb. 2004.

[7] A. Hoover and M. Goldbaum, "Locating the optic nerve in a retinal image using the fuzzy convergence of the blood vessels," *IEEE Trans. Med. Imag.*, vol. 22, no. 8, pp. 951–958, Aug. 2003.

[8] A. Aquino, M. E. Gegündez-Arias, and D. Marin, "Detecting the Optic Disc Boundary in Digital Fundus Images Using Morphological, Edge Detection, and Feature Extraction Techniques," *IEEE Trans. Med. Imag.*, vol. 29, no. 11, pp. 1860-1869 , 2010.

[9] H. A. Quigley and A. T. Broman, "The number of people with glaucoma worldwide in 2010 and 2020," *Br. J. Ophthalmol.*, vol. 90, pp. 262–267, 2006.